INFECTION AND IMMUNITY, May 1994, p. 1768–1775
0019-9567/94/$04.00+0

Vol. 62, No. 5

Evidence that the A_2 Fragment of Shiga-Like Toxin Type I Is Required for Holotoxin Integrity

PAULA R. AUSTIN,[1] PETER E. JABLONSKI,[1] GREGORY A. BOHACH,[1] A. KEITH DUNKER,[2] AND CAROLYN J. HOVDE[1]*

Department of Microbiology, Molecular Biology, and Biochemistry, University of Idaho, Moscow, Idaho 83843,[1] and Department of Biochemistry and Biophysics, Washington State University, Pullman, Washington 99164-4660[2]

Received 27 December 1993/Returned for modification 4 February 1994/Accepted 25 February 1994

***Escherichia coli* Shiga-like toxin type I (SLT-I) is a potent cytotoxin consisting of an enzymatically active A subunit and a pentameric B subunit that mediates toxin binding to susceptible eukaryotic cells. Evidence that the carboxy-terminal 38 amino acids of the A subunit are involved in holotoxin 1A:5B association is presented. We compared the ability of purified recombinant SLT-I B subunit (Slt-IB) to combine in vitro with purified recombinant SLT-I A subunit (Slt-IA; full-length subunit A includes amino acids 1 to 293) and its ability to combine with purified recombinant SLT-I A_1 subunit (Slt-IA_1; truncated subunit A includes amino acids 1 to 255). Each mixture was analyzed for biological and physical evidence of toxin assembly. Although Slt-IA successfully combined with Slt-IB to form a molecular species similar to holotoxin that was detectable by nondenaturing polyacrylamide gel electrophoresis and immunoblotting and yielded a molecule which was cytotoxic to cultured Vero cells, Slt-IA_1 did not have this ability. Slt-IA_1 was 36-fold more active than Slt-IA in an in vitro protein synthesis inhibition assay. These findings suggest that the Slt-IA_2 fragment is crucial for formation of SLT holotoxin and stabilizes the interaction between the A and B subunits.**

Shiga-like toxins (SLTs) are potent cytotoxins produced by certain strains of pathogenic *Escherichia coli* which have been implicated in both human and animal disease (1, 32). For example, a recent hamburger-borne outbreak in the northwestern United States involved over 500 individuals and resulted in infectious diseases ranging from uncomplicated diarrhea to serious conditions including hemorrhagic colitis and hemolytic uremic syndrome (6). *E. coli* producing SLT(s) can also cause postweaning diarrhea in calves and edema disease of swine (7, 29).

Five SLTs have been described: SLT type I (SLT-I), SLT-I variant, SLT type II (SLT-II), and two SLT-II variants, SLT-IIva and SLT-IIe (previously called SLT-IIv) (13, 21, 29, 34). Because of similar biological, structural, and mechanistic features, the SLTs as well as Shiga toxin (STX) produced by *Shigella dysenteriae* are categorized as the Shiga toxin family (20). SLT-I and STX are immunologically cross-reactive and toxic to Vero cells at similar doses (32). Three independent determinations of the SLT-I amino acid sequence, deduced from nucleotide sequences, showed SLT-I to be 99% identical to STX (5, 8, 21). It has also been reported that the amino acid sequences of STX and SLT-I are identical (44). SLT-II, SLT-IIva, and SLT-IIe share approximately 60% amino acid sequence similarity with SLT-I and are cytotoxic to Vero cells but are immunologically distinct from SLT-I (13, 21, 47). STX, SLT-I, and SLT-II bind to the cell surface receptor globotriosylceramide, whereas the receptor for SLT-IIva and SLT-IIe is globotetraosylceramide (9, 13, 19, 27, 46).

Members of the Shiga toxin family are bipartite molecules composed of a single enzymatically active A subunit noncovalently associated with a pentamer of receptor-binding B subunits. Holotoxin, bound to surface receptors of susceptible eukaryotic cells, is internalized by receptor-mediated endocytosis (22, 32). Through mechanisms not yet understood, the A subunit or a catalytic fragment reaches substrate ribosomes in the cytosol (33, 38). Studies suggest that toxin trafficking includes movement of the STX A subunit (STX-A) into the Golgi apparatus (38). In vitro analyses of SLT-I A subunit (Slt-IA) have shown that mild proteolysis and reduction yield two smaller fragments: A_1 (Slt-IA_1; molecular weight, 27,000), which retains enzymatic activity, and noncatalytic A_2 (Slt-IA_2; molecular weight, 3,000), which is located at the C-terminal end of the A subunit (1, 3, 32). Potential protease sites in Slt-IA are residues 248 and/or 251, and resolution of two fragments requires reduction of the disulfide bond that connects cysteine residues at positions 242 and 261 (5). The enzymatic mechanism of the Shiga family toxins is well characterized. All are single-site RNA *N*-glycosidases which specifically depurinate 28S rRNA (A_{4324} in rat liver rRNA), preventing elongation factor I-dependent binding of aminoacyl-tRNAs to 60S ribosomal subunits (25, 35, 39). The resulting inhibition of protein synthesis ultimately causes the death of intoxicated cells (35).

Several diverse bacterial toxins with unique mechanisms of cell entry and enzymology share the 1A:5B structural motif with the Shiga toxin family. These include cholera toxin (CT) from *Vibrio cholera*, heat-labile toxin (LT) from *E. coli*, and pertussis toxin (PT) from *Bordetella pertussis* (14, 41, 45). Crystal structures of CT, LT, SLT-I B subunit (Slt-IB) pentamer, and, most recently, STX holotoxin have been determined (12, 36, 40, 41). There are striking structural similarities among these toxins that include the length of their A_2 fragments, the doughnut-shaped ring of B subunits, and an oligosaccharide binding-fold in the B subunit of several of the toxins (12, 30, 36, 40, 41). Despite these shared properties, computer-assisted alignments of the amino acid sequence of SLT-I with the sequences of CT, LT, and PT do not reveal significant similarities (5, 8, 28, 31). The Slt-IB pentamer crystal structure

* Corresponding author. Mailing address: Department of Microbiology, Molecular Biology, and Biochemistry, University of Idaho, Moscow, ID 83843. Phone: (208) 885-5906. Fax: (208) 885-6518. Electronic mail address: cbohach@crow.csrv.uidaho.edu.

contains a pore which is lined by neutral and nonpolar residues, which is in contrast to the highly charged pore of the LT pentameric B subunit pore (41, 43). Since it has been shown that amino acids in the A_2 fragments of CT and LT are involved in their respective holotoxin integrities, we, as others (14, 41), hypothesized that the A_2 fragment of SLT-I has an analogous function. The purpose of this study was to assess the contribution of A_2 in SLT-I holotoxin formation. By using previously engineered constructs for the expression of Slt-IA, Slt-IA_1, or Slt-IB, we demonstrated that the Slt-IA_2 fragment is required for subunit association.

MATERIALS AND METHODS

Strains and plasmids. Three strains of *E. coli* were used in this study: JM105 [*thi-1 rpsL endA sbcB15 hsdR4* Δ(*lac-proAB*) (F′ *traD36 proAB lacI*^{q}*Z*ΔM15)], DH5α [F$^-$ ϕ80d*lacZ*ΔM15 *recA1 endA1 gyrA96 thi-1 hsdR17* ($r_K^-m_K^+$) *supE44 relA1 deoR* Δ(*lacZYA-argF*)*U169*], and SY327 [F$^-$ *araD* Δ(*lac-pro*) *argE(Am) rif nalA recA56*] (15). Plasmid pSC25, which encodes the intact *slt*-IA gene and a truncated portion of the *slt*-IB gene, was expressed in *E. coli* SY327 (5). Plasmid pRD500, which encodes the signal sequence and the 255 N-terminal residues of Slt-IA, was expressed in DH5α (10). Briefly, the PCR was used to introduce a stop codon directly after the codon for the residue at position 255 in mature Slt-IA. The gene product of this construct is a good approximation of Slt-IA_1, whose length is unknown and has been estimated to be the N-terminal 253, 251, or 248 amino acids (5, 10, 24, 44). The expression of these genes was under the control of the *lacZ* promoter of pUC19. Plasmid pSBC32, which encodes the complete Slt-IB protein, was expressed under the control of the *trc* promoter of pKK233-2 in JM105 (4).

Media and growth conditions. All *E. coli* cultures were grown for 18 h (37°C) in Luria-Bertani (LB) medium (37) containing 100 μg of ampicillin (Sigma Chemical Co., St. Louis, Mo.) per ml, and 4 ml was used to inoculate 1 liter of fresh medium. Cultures were grown to the late exponential growth phase and harvested by centrifugation at 12,000 × *g* for 15 min at 4°C.

Purification of recombinant Slt-IA, Slt-IA_1, and Slt-IB. Recombinant Slt-IA or Slt-IA_1 was purified by dye-ligand affinity chromatography as described previously (49). Briefly, Slt-IA or Slt-IA_1 was released from the periplasm of *E. coli* SY327(pSC25) or *E. coli* DH5α(pRD500), respectively, by using polymyxin B sulfate. Toxin subunits were precipitated with ammonium sulfate, adsorbed to a Matrex Gel Green A dye-ligand agarose column (Amicon Corp., Lexington, Mass.), and eluted as a single peak of protein with approximately 0.3 M NaCl.

Slt-IB was purified by a previously unreported procedure. Recombinant Slt-IB was released from the periplasm of *E. coli* JM105(pSBC32), an Slt-IA-negative strain, with polymyxin B sulfate, by the procedure used for the release of Slt-IA and Slt-IA_1 (49). Cells from a 1-liter culture were resuspended in 100 ml of 50 mM sodium phosphate buffer (pH 7.4) containing 140 mM NaCl and 200 mg of polymyxin B sulfate (7,730 USP units/mg; Sigma). The suspension was incubated on ice for 20 min and centrifuged at 16,000 × *g* for 10 min at 4°C. The supernatant was collected, and solid ammonium sulfate was added at 0°C to achieve 80% saturation (523 g/liter). The resulting precipitate was recovered by centrifugation at 16,000 × *g* for 20 min at 4°C. The pellet was dissolved in 9 ml of 50 mM sodium phosphate buffer (pH 7.4; 9 ml) and then dialyzed against 4 liters of 10 mM sodium phosphate buffer (pH 7.4) for 16 h at 4°C. Slt-IB was partially purified by isoelectric focusing (IEF) with a Rotofor preparative cell (Bio-Rad Laboratories, Hercules, Calif.). The dialyzed protein was diluted to 55 ml in deionized water containing 2% 3/10 Bio-lyte ampholytes (Bio-Rad) and 1% glycerol (Aldrich Chemical Co., Milwaukee, Wis.) and focused at a constant power of 12 W for 5 h at 4°C. The equilibrium voltage was approximately 700 V. Twenty fractions were harvested as described in the protocol of the manufacturer, and the pH values were determined by using an Alkacid full-range pH kit (Fisher Scientific Co., Pittsburgh, Pa.). Fractions containing Slt-IB were pooled, refocused, and harvested as described above without further addition of ampholytes or glycerol. The voltage at equilibrium was approximately 2,700 V. The protein content of each fraction was analyzed by sodium dodecyl sulfate-polyacrylamide gel electrophoresis (SDS-PAGE; 18% polyacrylamide gels) by the method of Laemmli (26) and stained with silver (2). Immunoreactive bands were detected by immunoblotting with rabbit anti-STX-B or anti-STX sera (kindly provided by A. Donohue-Rolfe, Tufts University School of Medicine, Boston, Mass.). After the refocusing procedure was performed, fractions containing SLT-IB were pooled and concentrated to approximately 1 ml by using solid polyethylene glycol compound (molecular weight, 15,000 to 20,000; Sigma) (23). The purity of Slt-IB was estimated by using densitometry of silver-stained SDS-polyacrylamide gels (2, 26). The protein concentration was determined by using a commercially available kit (Bio-Rad) with bovine serum albumin (Sigma) as a standard.

Assay of Slt-IA and Slt-IA_1 enzymatic activity. Purified Slt-IA or Slt-IA_1 was analyzed for the ability to inhibit protein synthesis in a cell-free system with rabbit reticulocyte lysate and brome mosaic virus as mRNA (Promega Corp., Madison, Wis.) as described previously (10). Extracts were diluted in ice-cold 100 mM potassium acetate buffer (pH 7.4) and preincubated with reticulocyte lysate at 30°C for 20 min to inactivate ribosomes prior to the addition of amino acids, [^{35}S]methionine, and mRNA. The reaction mixture (25.5 μl) contained 0.04 mM amino acid mixture (without methionine), 20 μCi of [^{35}S]methionine (NEN Research Products, Boston, Mass.), and 500 ng of mRNA. Reaction mixtures were incubated at 30°C for 30 min. Incorporation of radiolabel into alkali-resistant, trichloroacetic acid-precipitable material was determined as described by the manufacturer. For the negative control, mRNA was omitted. Activity was expressed as a percentage of [^{35}S]methionine in acid-precipitable material compared with that in the positive control (reticulocyte lysate preincubated with buffer only).

In vitro subunit association. Purified Slt-IA and Slt-IA_1 were diluted to 0.1 μM in 10 mM Tris-HCl (pH 7.0). Purified Slt-IB was diluted to 1.0 μM in the same buffer. Slt-IA or Slt-IA_1 (500 μl) was combined with an equal volume (10-fold molar excess) of Slt-IB in Spectra/Por 3 dialysis tubing (Spectrum Medical Industries, Inc., Houston, Tex.) with a 3,500-molecular-weight cutoff and dialyzed against 10 mM Tris-HCl (pH 7.0) for 16 h at 4°C (18). Similarly, Slt-IA, Slt-IA_1, and Slt-IB were dialyzed individually. To confirm that the Slt-IA_1 preparation did not contain a spurious inhibitor of subunit association, all three subunits, i.e., Slt-IA, Slt-IA_1, and Slt-IB (500 μl each), were combined and dialyzed as described above. Subunit association was analyzed by discontinuous native PAGE (8% polyacrylamide gels) as described above except that SDS was not present in any of the solutions. Proteins were visualized by staining with silver or by immunoblotting as described above.

Analysis of in vitro cytotoxicity. Each subunit preparation

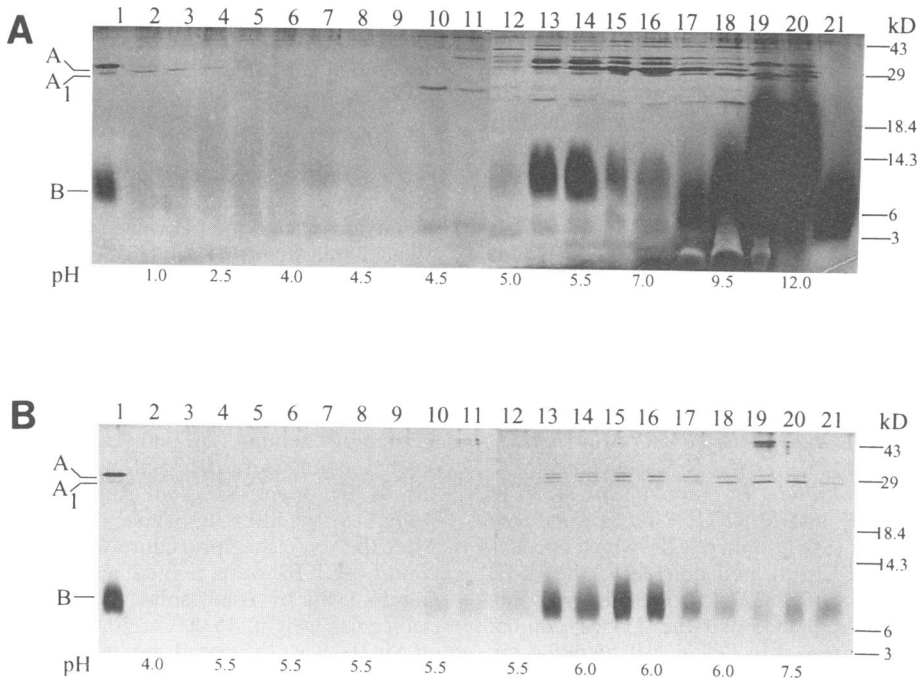

FIG. 1. SDS-PAGE analysis of Slt-IB purified by IEF. (A) Analysis of IEF in a pH gradient of 3 to 10. Fractions containing Slt-IB (i.e., 13 through 16) were refocused in a narrow gradient. (B) Analysis of refocused IEF fractions. Lanes: 1, STX; 2 to 21, fractions 1 to 20, respectively. The positions of STX-A, -A_1, and -B are indicated to the left of each gel. The pH values of selected fractions are shown along the bottom of each panel. Molecular mass marker positions are indicated to the right of both gels.

was analyzed for toxicity to African green monkey kidney cells (referred to as Vero cells; CCL81; American Type Culture Collection, Rockville, Md.) by using an adaptation of the in vitro cytotoxicity assay of Konowalchuk and colleagues (25). Vero cells were incubated in 96-well microtiter plates (Falcon Labware, Lincoln Park, N.J.) for approximately 48 h (37°C in a 5% CO_2 atmosphere) to achieve 85% cell confluence. All experiments were performed with cultures grown in medium 199 (pH 7.4; Gibco-BRL Laboratories, Grand Island, N.Y.) supplemented with 5% (vol/vol) heat-inactivated fetal bovine serum (HyClone Laboratories Inc., Logan, Utah), 1% (wt/vol) (each) penicillin and streptomycin (Gibco-BRL), and 0.22% (wt/vol) sodium bicarbonate (tissue culture grade; Gibco-BRL). To compare their toxicities, 10-fold serial dilutions of combined or individual toxin subunits were prepared in complete medium 199 and added (25 μl) to the cell cultures. All assays were performed in triplicate. Pure STX, used as a positive control, was a gift from A. Donohue-Rolfe. The resulting preparations were incubated for 72 h, and the percent viability of cells was determined by microscopic observation for cytopathology as described by Konowalchuk et al. (25) and Speirs et al. (42).

RESULTS

Toxin subunit expression and purification. Recombinant Slt-IA, Slt-IA_1, and Slt-IB were overexpressed in *E. coli* by using plasmid expression vectors. Slt-IA, Slt-IA_1, and Slt-IB were released from the periplasm of *E. coli* clones by using polymyxin B sulfate in a procedure frequently employed for the isolation of Shiga toxin family members or their subunits (11, 16, 23). Slt-IA and Slt-IA_1 were purified to homogeneity (results not shown) by Matrex Gel Green A dye-ligand affinity chromatography as described previously (49).

Slt-IB was purified by a novel three-step protocol. In the last step, preparative IEF, this subunit focused in fractions with pH values between 5.5 and 6.0, which is consistent with the previously reported pI for SLT-IB (Fig. 1) (48). The identity of Slt-IB was confirmed by immunoblotting (results not shown). In SDS-PAGE, Slt-IB resolved as a low-molecular-mass protein of approximately 7,000 Da, with a broad migration pattern, as reported by others (4). This purification procedure routinely resulted in approximately 1 mg of Slt-IB purified to at least 97% homogeneity from a 1-liter culture.

Enzymatic activity of Slt-IA and Slt-IA_1. Purified Slt-IA or Slt-IA_1 was analyzed for the capacity to inhibit protein synthesis in a cell-free translation system. Results from a representative experiment in which Slt-IA_1 or Slt-IA was highly active are shown in Fig. 2. Purified Slt-IA_1, at a concentration of 0.05 fM, inhibited protein synthesis by 50%, while approximately 36-fold more (1.8 fM) purified Slt-IA was required for the same level of inhibition. Therefore, similar to the results obtained when STX-A and STX-A_1 were compared (33, 35), Slt-IA_1 was more active than Slt-IA at inhibiting protein synthesis. This result is in agreement with previous reports; however, we report an even greater difference in activity.

Analysis of subunit association. Purified SLT subunits were mixed in vitro to determine their ability to form a complex analogous to the holotoxin. Subunit assembly was analyzed by native PAGE and reactivity of the products with either anti-STX sera or anti-STX-B (Fig. 3). Separation of proteins in nondenaturing gels is not dependent on size but on a combination of physical features that includes charge, molecular weight, and native shape. The preparation of anti-STX used in all assays bound very weakly to the Slt-IB subunit alone; however, it bound well to Slt-IA_1 (Fig. 3A) and Slt-IA in denaturing SDS-PAGE (data not shown). Full-length Slt-IA was able to bind with Slt-IB (Fig. 3, lanes 8), whereas no

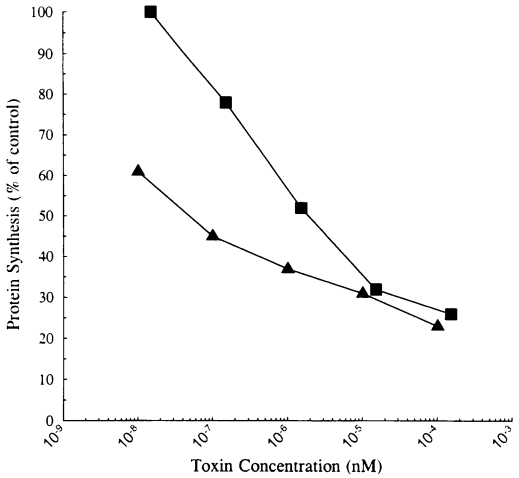

FIG. 2. Inhibition of protein synthesis by Slt-IA (■) or Slt-IA_1 (▲). Aliquots of a rabbit reticulocyte lysate were preincubated with purified Slt-IA or Slt-IA_1 at the concentrations indicated. The lysates were assessed for the ability to synthesize protein and compared with control lysates preincubated with buffer only. Background activity (mRNA omitted) was subtracted from each value. Control lysate total counts were 6.9×10^5 to 7.2×10^5 cpm and background total counts were 2×10^3 to 3.5×10^3 cpm. Datum points shown are the means from three assays.

interaction of Slt-IA_1 with Slt-IB could be detected (Fig. 3, lanes 4). Anti-STX sera reacted with STX holotoxin (Fig. 3A, lanes 1 and 5) and with a molecular species representing combined Slt-IA and Slt-IB (Fig. 3A, lane 8). In contrast, an analogous holotoxin band was not seen in mixtures of Slt-IA_1 and Slt-IB (Fig. 3A, lane 4). Although the presence of Slt-IA in the sample was confirmed by denaturing SDS-PAGE (results not shown), Slt-IA was not detectable in native gels (Fig. 3A, lane 6). This is most likely due to the strong positive charge of the full-length SLT-I A chain (49) preventing its migration towards the anode under the gel conditions of pH 8.8. Similar results were seen when anti-STX-B serum was used to develop identical immunoblots. A strong reaction was seen with STX holotoxin and to a protein with a similar position in the gel when Slt-IA and Slt-IB were combined but not in mixtures of Slt-IA_1 and Slt-IB (Fig. 3B, lanes 8 and 4). Anti-STX-B also bound to dissociated B subunit. As expected, anti-STX-B did not cross-react with Slt-IA_1 (Fig. 3B, lane 2) nor with Slt-IA in SDS-polyacrylamide gels (data not shown).

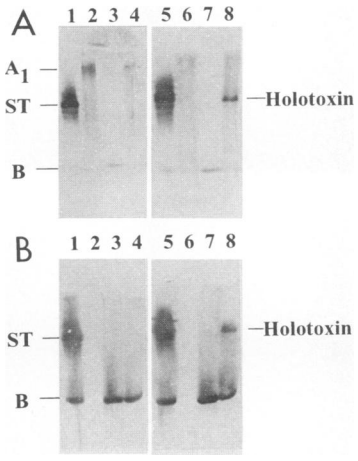

FIG. 3. Nondenaturing PAGE of SLT subunit reconstitution. Samples of combined or individual subunits were electrophoresed under nondenaturing conditions through an 8% polyacrylamide gel, electroblotted onto nitrocellulose, and probed with anti-STX (A) or anti-STX-B (B). Lanes: 1 and 5, STX; 2, Slt-IA_1; 3 and 7, Slt-IB; 4, Slt-IA_1–Slt-IB; 6, Slt-IA; 8, Slt-IA–Slt-IB. The positions of STX (ST), the B subunit (B), and the A_1 subunit (A_1) are indicated to the left of the gels. The position of a molecular species in the Slt-IA–Slt-IB mixture that reacted with both antisera and migrated at a position similar to that of STX (holotoxin) is indicated to the right.

Analysis of cytotoxicity. To further investigate the ability of SLT subunits to combine in vitro, individual and mixed subunits were analyzed for their cytotoxicity to Vero cells. This assay could be a sensitive indicator of subunit association since holotoxin is required for toxicity and is lethal at very low levels (23). Cytotoxicity was evaluated by light microscopy, and the percentage of viable cells was determined after 72 h of incubation.

These results confirm the observations obtained by native gel immunoblots that Slt-IA, but not Slt-IA_1, recombined with Slt-IB (Fig. 4C and B, respectively). As expected, neither Slt-IB, Slt-IA, nor Slt-IA_1 subunits alone were cytotoxic (Fig. 4G, F, and E, respectively). Vero cells incubated with STX control (Fig. 4A) or mixtures of Slt-IA and Slt-IB (Fig. 4C) appeared rounded and had detached from the microtiter plate, indicating that a functional holotoxin had formed. In contrast, Vero cells incubated with mixtures of Slt-IA_1 and Slt-IB (Fig. 4B) retained a healthy appearance, i.e., flattened elongated cells that strongly attached to the microtiter plate. This lack of cytotoxicity was not attributed to loss of enzymatic activity since Slt-IA and Slt-IA_1 were both active (see "Enzymatic activity of Slt-IA and Slt-IA_1" above). This confirmed that the association of receptor-binding Slt-IB with an enzymatically active subunit is required for cell intoxication and only occurred with Slt-IA. Mixtures containing all three subunits, i.e., Slt-IA, Slt-IA_1, and Slt-IB (Fig. 4D), were toxic to Vero cells, indicating that the preparations of Slt-IA_1 did not contain a spurious inhibitor of subunit association.

While mixtures of Slt-IA_1 and Slt-IB were not toxic to Vero cells, mixtures of Slt-IA and Slt-IB were toxic to Vero cells at concentrations as low as 10^{-7} μM and had a potency comparable to that of native STX at concentrations as low as 10^{-5} μM. For example, at concentrations of 10^{-5} μM, the percentages of viable cells after incubation with STX or Slt-IA–Slt-IB mixtures were 19 and 13%, respectively (Fig. 5). In sharp contrast, when treated with the same concentration of Slt-IA_1–Slt-IB mixture, 94% of the cells remained viable; at very high concentrations (10^{-1} μM), only minimal cytotoxicity was evident. This effect was not due to a spurious inhibitor of cytotoxicity in the Slt-IA_1 preparations because, after incubation with 10^{-6} μM Slt-IA_1–Slt-IA–Slt-IB mixtures, only 22% of the cells remained viable. Cells incubated with all preparations of single subunits remained at least 86% viable for the 72-h experimental period.

DISCUSSION

SLT-I is a bipartite molecule composed of a single enzymatically active A subunit noncovalently associated with a pentamer of receptor-binding B subunits. The purpose of this investigation was to compare the abilities of Slt-IA and Slt-IA_1 to associate with Slt-IB. The experimental strategy involved a determination of whether SLT-I holotoxin was formed upon mixing either the full-length Slt-IA or truncated Slt-IA, generated by a C-terminal deletion (Slt-IA_1), with Slt-IB. Recombi-

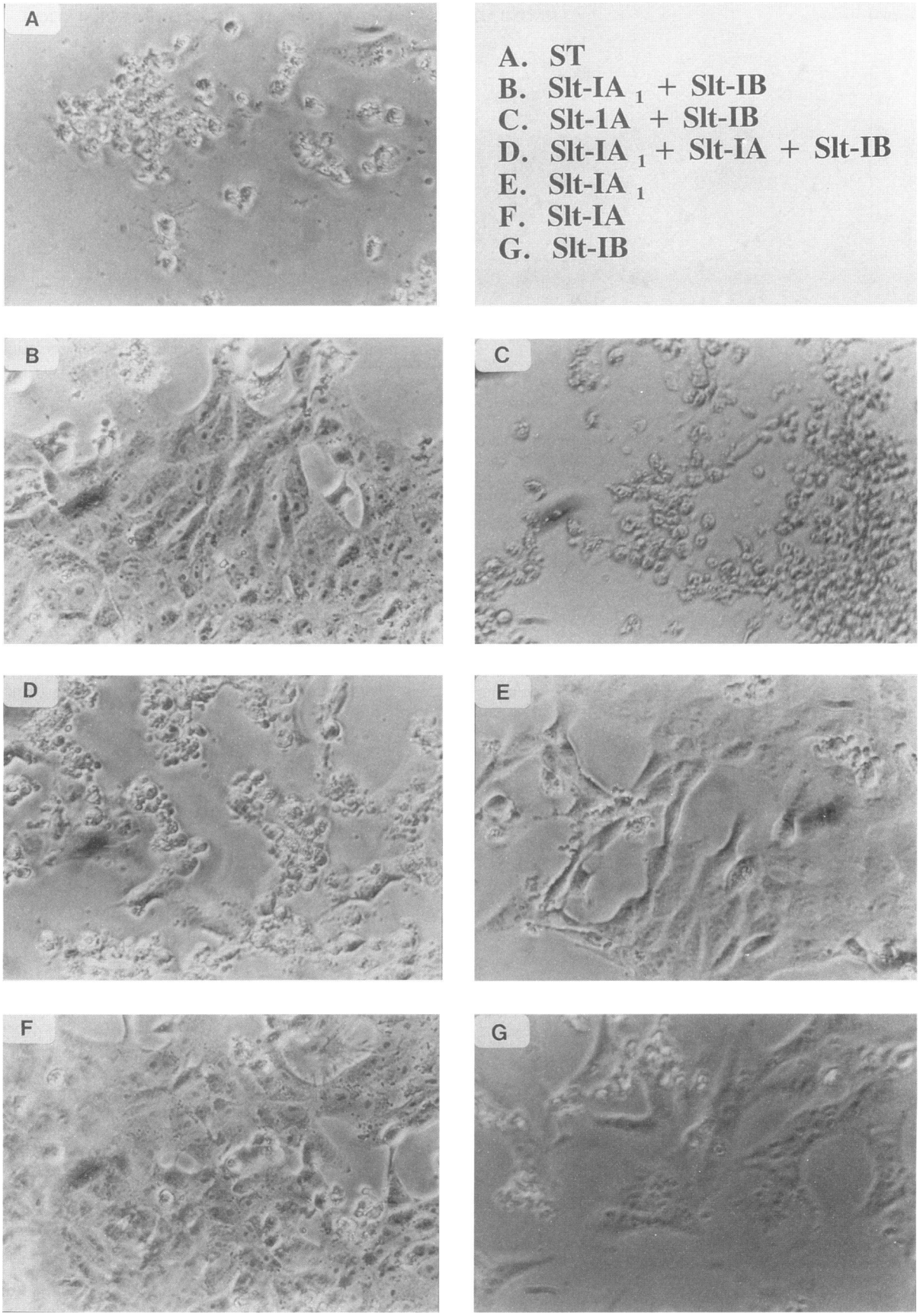

FIG. 4. Effect of toxin and subunits on Vero cells. Vero cell monolayer cultures were exposed to each preparation (1.0 nM) for 72 h and viewed by phase-contrast microscopy (200×). Rounded and refractive cells, typical evidence of cytopathic effects of the toxin, are seen in panels A, C, and D. Flattened and elongated cells, typical of healthy cells, are seen in panels B, E, F, and G.

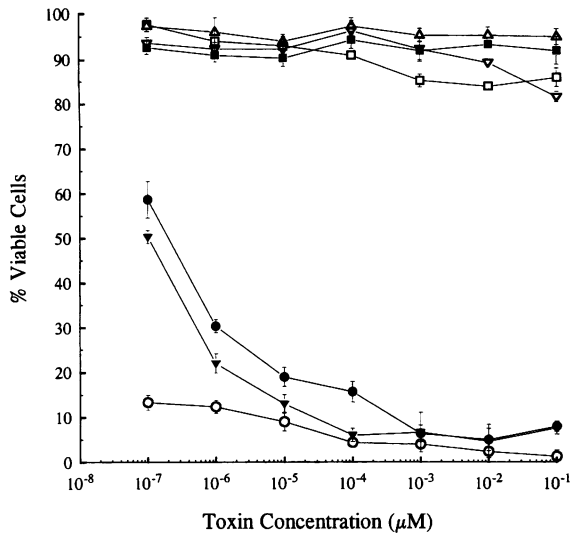

FIG. 5. Quantitation of Vero cell viability after incubation with toxin or subunits. Individual or mixed subunits were incubated with Vero cells for 72 h at the protein concentration (micromolar) shown. Cell viability was determined microscopically and expressed as a percentage (at least 300 cells per reaction were counted in each culture). Data shown are the means (±standard errors of the means) of triplicate cultures. Symbols: ○, STX; ●, Slt-IA–Slt-IB; ▽, Slt-IA_1–Slt-IB; ▼, Slt-IA_1–Slt-IA–Slt-IB; □, Slt-IA; ■, Slt-IA_1; △, Slt-IB.

nant Slt-IA, Slt-IA_1, and Slt-IB subunits were used in this study. The Slt-IB purification protocol used has not been reported previously, and this simple three-stage procedure offers several advantages over other commonly used methods (3, 39). Formation of a functional holotoxin was evaluated by both physical and biological methods. Although full-length subunit A, which contains 293 amino acids, readily associated with Slt-IB, Slt-IA_1, consisting of the first 255 amino acids of the A chain, did not have this ability. These results provide evidence that the carboxy-terminal 38 amino acids of the SLT A subunit are involved in holotoxin integrity and appear to interact directly with the B subunits.

The requirement of an intact A subunit has been demonstrated with several other bacterial toxins. Although their amino acid sequences and pathogenic mechanisms differ from those of the Shiga toxin family, CT and *E. coli* LT have several structural features in common with SLT-I. The functional topology of the six subunits in each of these bacterial exotoxins, which contain one A (enzymatic) subunit and five B (receptor-binding) subunits, is organized similarly. As early as 1976, Gill determined that CT A_2 subunit (CT-A_2) is necessary for the assembly of CT holotoxin (14). More recent X-ray crystallography data have demonstrated that residues of LT A_2 subunit (LT-A_2) thread through a central pore formed by the B pentamer (41). The LT-B pentamer, which is responsible for binding to the ganglioside saccharide receptors on the outer surface of the epithelial cells of the intestinal tract in the human host, has a ring shape with a central pore (41). The pore is lined by the amphipathic α2 helices of the five subunits (41). The pore has a very polar and charged surface, while the hydrophobic side chains of the helices are directed towards the interior of the molecule (41). The association of the A subunit with the B pentamer involves the C-terminal half of the LT-A_2 fragment (41). The residues that can be resolved are in an extended conformation in the pore of LT (41).

More recent crystallographic analyses are consistent with our finding that Slt-IA_2 is necessary for SLT holotoxin formation but that the interaction of Slt-IA_2 with Slt-IB is unique in comparison with subunit interactions in LT (12, 41, 43). In 1992, the crystal structure of the SLT-I B oligomer, without the A subunit, was solved (43). Although its ring structure arrangement resembles that of the LT-B oligomer, and it was suspected that the A_2 fragment of Slt-IA could be involved in holotoxin integrity, the Slt-IB pentamer pore is lined by neutral and nonpolar residues (43). Therefore, unlike the ionic interactions between LT-A and LT-B, it was proposed that hydrophobic residues in Slt-IA_2 would interact with the nonpolar and hydrophobic residues lining the Slt-IB pentamer pore (41, 43). Consistent with this prediction is the fact that approximately 50% of the Slt-IA_2 primary sequence consists of a hydrophobic stretch of 19 residues encompassing positions 275 through 293. Finally, the more recent resolution of the crystal structure for the highly related STX holotoxin has shown that its five B subunits form a pentameric ring encircling a C-terminal α-helix of STX-A (12). The rest of STX-A sits on the face of the ring.

Prior investigations into the effect of the C terminus of STX-A on enzymatic activity have produced conflicting results. Although STX-A_1 was initially reported to be at least sixfold more active than STX-A (35), Haddad et al. found that deletion of 22 C-terminal residues of the same protein resulted in a 30% decrease in enzymatic activity (17). In the present study, the data obtained by comparing the activity of Slt-IA and Slt-IA_1 are consistent with those of the former study. Removal of Slt-IA_2 augmented the enzymatic inhibition of protein synthesis. To confirm that the lack of cytotoxicity seen in mixtures of Slt-IA_1 and Slt-IB could not be explained by a lack or reduction of catalytic activity, the effects of Slt-IA and Slt-IA_1 on in vitro protein synthesis were compared. Our observed 36-fold increase in activity of Slt-IA_1 compared with that of Slt-IA is most likely due to the deletion of methionine-260, since the side chain of this residue is oriented into the active site of the enzyme (12).

More recently, however, Haddad et al. have also provided evidence that STX-A_2 is required for STX holotoxin assembly (17). Their data is in full agreement with our results. These investigators, by utilizing mutant STX-A, implicated a stretch of nine nonpolar amino acids (residues 279 and 287) near the C terminus of STX-A that were required for A-B subunit association. They proposed a model in which these nine residues penetrate the B pentamer pore and indicate that amino acids at the boundaries of this sequence may stabilize the noncovalent subunit association through interactions with amino acids outside the neutral pore of the B subunit pentamer.

ACKNOWLEDGMENTS

We thank Arthur Donohue-Rolfe for providing us with anti-STX serum, anti-STX-B serum, and purified STX. We also acknowledge Marie Faser and Michael James for helpful discussions of the STX crystal structure.

This study was supported in part by the Idaho Agriculture Experiment Station, the U.S. Department of Agriculture grant 92-04350, the Public Health Service grant AI33981 from the National Institutes of Health, the Idaho Beef Council grant 91545, and a United Dairymen of Idaho grant.

REFERENCES

1. **Acheson, D. W. K., A. Donohue-Rolfe, and G. T. Keusch.** 1991. The family of Shiga and Shiga-like toxins, p. 415–433. *In* J. E. Alouf and J. H. Freer (ed.), Sourcebook of bacterial toxins. Academic Press Ltd., London.

2. **Blum, H., H. Beier, and H. J. Gross.** 1987. Improved silver staining of plant proteins, RNA and DNA in polyacrylamide gels. Electrophoresis **8**:93–94.
3. **Brown, J. E., M. A. Ussery, S. H. Leppla, and S. W. Rothman.** 1980. Inhibition of protein synthesis by Shiga toxin. Activation of the toxin and inhibition of peptide elongation. FEBS Lett. **117**: 84–88.
4. **Calderwood, S. B., D. W. K. Acheson, M. B. Goldberg, S. A. Boyko, and A. Donohue-Rolfe.** 1990. A system for production and rapid purification of large amounts of the Shiga toxin/Shiga-like toxin I B subunit. Infect. Immun. **58**:2977–2982.
5. **Calderwood, S. B., F. Auclair, A. Donohue-Rolfe, G. T. Keusch, and J. J. Mekalanos.** 1987. Nucleotide sequence of the Shiga-like toxin genes of *Escherichia coli*. Proc. Natl. Acad. Sci. USA **84**:4364–4368.
6. **Centers for Disease Control and Prevention.** 1993. Update: multistate outbreak of *Escherichia coli* O157:H7 infections from hamburgers—Western United States, 1992–1993. Morbid. Mortal. Weekly Rep. **42**:258–263.
7. **Chanter, N., G. A. Hall, A. P. Bland, A. J. Hayle, and K. R. Parsons.** 1986. Dysentery in calves caused by an atypical strain of *Escherichia coli* (S102-9). Vet. Microbiol. **12**:241–253.
8. **DeGrandis, S., J. Ginsberg, M. Toone, S. Climie, J. Friesen, and J. Brunton.** 1987. Nucleotide sequence and promoter mapping of the *Escherichia coli* Shiga-like toxin operon of bacteriophage H-19B. J. Bacteriol. **169**:4313–4319.
9. **DeGrandis, S., H. Law, J. Brunton, C. Gyles, and C. A. Lingwood.** 1989. Globotetraosylceramide is recognized by the pig edema disease toxin. J. Biol. Chem. **264**:12520–12525.
10. **Deresiewicz, R. L., P. R. Austin, and C. J. Hovde.** 1993. The role of tyrosine-114 in the enzymatic activity of the Shiga-like toxin I A-chain. Mol. Gen. Genet. **241**:467–473.
11. **Donohue-Rolfe, A., and G. T. Keusch.** 1983. *Shigella dysenteriae* 1 cytotoxin: periplasmic protein release by polymyxin B and osmotic shock. Infect. Immun. **39**:270–274.
12. **Fraser, M. E., M. M. Chernaia, Y. V. Kozlov, and M. N. G. James.** X-ray crystal structure of the holotoxin from *Shigella dysenteriae* at 2.5Å resolution. Nat. Struct. Biol., in press.
13. **Gannon, V. P. J., C. Teerling, S. A. Masri, and C. L. Gyles.** 1990. Molecular cloning and nucleotide sequence of another variant of the *Escherichia coli* Shiga-like toxin II family. J. Gen. Microbiol. **136**:1125–1135.
14. **Gill, D. M.** 1976. The arrangement of subunits in cholera toxin. Biochemistry **15**:1242–1248.
15. **Goldberg, I., and J. J. Mekalanos.** 1986. Cloning of the *Vibrio cholerae recA* gene and construction of a *Vibrio cholerae recA* mutant. J. Bacteriol. **165**:715–722.
16. **Griffin, D. E., and P. Gemski.** 1983. Release of Shiga toxin from *Shigella dysenteriae* 1 by polymyxin B. Infect. Immun. **40**:425–428.
17. **Haddad, J. E., A. Y. Al-Jaufy, and M. P. Jackson.** 1993. Minimum domain of the Shiga toxin A subunit required for enzymatic activity. J. Bacteriol. **175**:4970–4978.
18. **Ito, H., T. Yutsudo, T. Hirayama, and Y. Takeda.** 1988. Isolation and some properties of A and B subunits of Vero toxin 2 and *in vitro* formation of hybrid toxins between subunits of Vero toxin 1 and Vero toxin 2 from *Escherichia coli* O157:H7. Microb. Pathog. **5**:189–195.
19. **Jacewicz, M., H. Clausen, E. Nudelman, A. Donohue-Rolfe, and G. T. Keusch.** 1986. Pathogenesis of Shigella diarrhea. XI. Isolation of a Shigella toxin-binding glycolipid from rabbit jejunum and HeLa cells and its identification as globotriaosylceramide. J. Exp. Med. **163**:1391–1404.
20. **Jackson, M.** 1990. Structure-function analyses of Shiga toxin and the Shiga-like toxins. Microb. Pathog. **8**:235–242.
21. **Jackson, M. P., R. J. Neill, A. D. O'Brien, R. K. Holmes, and J. W. Newland.** 1987. Nucleotide sequence analysis and comparison of the structural genes for Shiga-like toxin I and Shiga-like toxin II encoded by bacteriophages from *Escherichia coli* 933. FEMS Microbiol. Lett. **44**:109–114.
22. **Keusch, G. T.** 1981. Receptor-mediated endocytosis of *Shigella* cytotoxin. Academic Press, Inc., New York.
23. **Keusch, G. T., A. Donohue-Rolfe, M. Jacewicz, and A. V. Kane.** 1988. Shiga toxin: production and purification. Methods Enzymol. **165**:152–162.
24. **Kittel, F. B., V. V. Padhye, and M. P. Doyle.** 1991. Characterization and inactivation of verotoxin 1 produced by *Escherichia coli* O157:H7. J. Agr. Food Chem. **39**:141–145.
25. **Konowalchuk, J., J. I. Speirs, and S. Stavric.** 1977. Vero response to a cytotoxin of *Escherichia coli*. Infect. Immun. **18**:775–779.
26. **Laemmli, U. K.** 1970. Cleavage of structural proteins during the assembly of the head of bacteriophage T4. Nature (London) **227**:680–685.
27. **Lindberg, A. A., J. E. Brown, N. Stromberg, M. Westling-Ryd, J. E. Schultz, and K. Karlson.** 1987. Identification of the carbohydrate receptors for Shiga toxin produced by *Shigella dysenteriae* type 1. J. Biol. Chem. **262**:1779–1785.
28. **Locht, C., and J. M. Keith.** 1986. Pertussis toxin gene: nucleotide sequence and genetic organization. Science **232**:1258–1264.
29. **Marques, L. R. M., J. S. M. Peiris, J. S. Cryz, and A. D. O'Brien.** 1987. *Escherichia coli* strains isolated from pigs with edema disease produce a variant of Shiga-like toxin II. FEMS Microbiol. Lett. **44**:33–38.
30. **Murzin, A. G.** 1993. OB(oligonucleotide/oligosaccharide binding)-fold: common structural and functional solution for non-homologous sequences. EMBO J. **12**:861–867.
31. **Nicosia, A., M. Perugini, C. Franzini, M. C. Casagli, M. G. Borri, G. Antoni, M. Almoni, P. Neri, G. Ratti, and R. Rappuoli.** 1986. Cloning and sequencing of the pertussis toxin genes: operon structure and gene duplication. Proc. Natl. Acad. Sci. USA **83**:4631–4635.
32. **O'Brien, A. D., and R. K. Holmes.** 1987. Shiga and Shiga-like toxins. Microbiol. Rev. **51**:206–220.
33. **Olsnes, S., R. Reisbig, and K. Eiklid.** 1981. Subunit structure of Shigella cytotoxin. J. Biol. Chem. **256**:8732–8738.
34. **Paton, A. W., J. C. Paton, P. N. Goldwater, M. W. Heuzenroeder, and P. A. Manning.** 1993. Sequence of a variant Shiga-like toxin type-I operon of *Escherichia coli* O111:H$^-$. Gene **129**:87–92.
35. **Reisbig, R., S. Olnes, and K. Eiklid.** 1981. The cytotoxic activity of Shigella toxin. Evidence for catalytic inactivation of the 60 S ribosomal subunit. J. Biol. Chem. **256**:8739–8744.
36. **Ribi, H. O., D. S. Ludwig, K. L. Mercer, G. K. Schoolnik, and R. D. Kornberg.** 1988. Three-dimensional structure of cholera toxin penetrating a lipid membrane. Science **239**:1272–1276.
37. **Sambrook, J., E. F. Fritsch, and T. Maniatis.** 1989. Molecular cloning: a laboratory manual. Cold Spring Harbor Laboratory Press, Cold Spring Harbor, N.Y.
38. **Sandvig, K., O. Garred, P. K. Holm, and B. van Deurs.** 1993. Endocytosis and intracellular transport of protein toxins. Biochem. Soc. Trans. **21**:707–711.
39. **Saxena, S. K., A. D. O'Brien, and E. J. Ackerman.** 1989. Shiga toxin, Shiga-like toxin II variant, and ricin are all single-site RNA *N*-glycosidases of 28S RNA when microinjected in *Xenopus* oocytes. J. Biol. Chem. **264**:596–601.
40. **Sixma, T. K., A. Aguirre, A. C. Terwisscha van Scheltinga, E. S. Wartna, K. H. Kalk, and W. G. J. Hol.** 1992. Heat-labile enterotoxin crystal forms with variable A/B_5 orientation. Analysis of conformational flexibility. FEBS Lett. **305**:81–85.
41. **Sixma, T. K., S. E. Pronk, K. H. Kalk, E. S. Wartna, B. A. M. van Zanten, B. Witholt, and W. G. J. Hol.** 1991. Crystal structure of a cholera toxin-related heat-labile enterotoxin from *E. coli*. Nature (London) **351**:371–377.
42. **Speirs, J. I., S. Stavric, and J. Konowalchuk.** 1977. Assay of *Escherichia coli* heat-labile enterotoxin with Vero cells. Infect. Immun. **16**:617–622.
43. **Stein, P. E., A. Boodhoo, G. J. Tyrrell, J. L. Brunton, and R. J. Read.** 1992. Crystal structure of the cell-binding B oligomer of verotoxin-1 from *E. coli*. Nature (London) **355**:748–750.
44. **Takao, T., T. Tanabe, Y. Hong, Y. Shimonishi, H. Kurazono, T. Yutsudo, C. Sasakawa, M. Yoshikawa, and Y. Takeda.** 1988. Identity of molecular structure of Shiga-like I (VT1) from *Escherichia coli* O157:H7 with that of Shiga toxin. Microb. Pathog. **5**:357–369.
45. **Tamura, M., K. Nogimori, S. Murai, M. Yajima, K. Ito, T. Katada,**

M. Ui, and S. Ishii. 1982. Subunit structure of islet-activating protein, pertussis toxin, in conformity with the A-B model. Biochemistry **21:**5516–5522.

46. **Waddell, T., S. Head, M. Petric, A. Cohen, and C. Lingwood.** 1988. Globotriosyl ceramide is specifically recognized by the *Escherichia coli* verocytotoxin 2. Biochem. Biophys. Res. Commun. **152:**674–679.
47. **Weinstein, D. L., M. P. Jackson, J. E. Samuel, R. K. Holmes, and A. D. O'Brien.** 1988. Cloning and sequencing of a Shiga-like toxin type II variant from an *Escherichia coli* strain responsible for edema disease of swine. J. Bacteriol. **170:**4223–4230.
48. **Yutsudo, T., T. Honda, T. Miwatani, and Y. Takeda.** 1987. Physiochemical characterization of A and B subunits of Shiga toxin and reconstitution of holotoxin from isolated subunits. Microbiol. Immunol. **31:**189–197.
49. **Zollman, T. M., P. R. Austin, P. E. Jablonski, and C. J. Hovde.** Purification of recombinant Shiga-like toxin type I A1 fragment from *Escherichia coli*. Protein Expression Purif., in press.